2014•2015
FACULTEIT GENEESKUNDE EN LEVENSWETENSCHAPPEN
master in de biomedische wetenschappen

Masterproef

Revealing interactions of differentiated dental pulp stem cells with a collagen type I hydrogel

Promotor :
dr. Wendy MARTENS

Sander Luyck

Proefschrift ingediend tot het behalen van de graad van master in de biomedische wetenschappen

De transnationale Universiteit Limburg is een uniek samenwerkingsverband van twee universiteiten in twee landen: de Universiteit Hasselt en Maastricht University.

universiteit hasselt
KNOWLEDGE IN ACTION

Universiteit Hasselt | Campus Hasselt | Martelarenlaan 42 | BE-3500 Hasselt
Universiteit Hasselt | Campus Diepenbeek | Agoralaan Gebouw D | BE-3590 Diepenbeek

universiteit hasselt | Maastricht University

2014•2015
FACULTEIT GENEESKUNDE EN LEVENSWETENSCHAPPEN
master in de biomedische wetenschappen

Masterproef

Revealing interactions of differentiated dental pulp stem cells with a collagen type I hydrogel

Promotor :
dr. Wendy MARTENS

Sander Luyck
Proefschrift ingediend tot het behalen van de graad van master in de biomedische wetenschappen

universiteit hasselt | Maastricht University

Table of contents

Acknowledgements

Over the last couple of months, I was able to participate in innovative stem cell research at the departments of Morphology and Biophysics at Hasselt University in order to complete my senior internship. Not only did I develop numerous skills, I was also encouraged to adopt proper scientist researcher qualities. Planning experiments, setting up protocols and thinking critically about the value and meaning of the collected results. Accordingly, I would like to thank every person that made this internship possible and making it an invaluable experience.

First of all I would like to thank my promotor dr. Wendy Martens for her guidance, support, and the moments of evaluation. I would also like to show a lot of gratitude to my daily supervisor Kathleen Sanen. Her guidance and valuable advice were indispensable and contributed significantly toward the development of my qualities as a researcher. In general, I would like to thank them both for the kindness and hospitality I experienced during my internship. I am truly grateful for the opportunity that I have been given.

Furthermore, I would also like to thank prof. dr. Ivo Lambrichts and prof. dr. Marcel Ameloot, who made it possible to do my internship here. My gratitude also goes out to dr. James Phillips for his input concerning the contraction experiments.

Finally, I would like to thank my parents and my girlfriend for their continuous support during my internship and thesis writing.

Sander Luyck; January 19th, 2015

List of abbreviations

- 3D 3-Dimensional
- α Alpha
- Ara-C Cytosine Arabinoside
- ASC Adult Stem Cell
- AT-MSCs Adipose Tissue-derived Mesenchymal Stem Cells
- β Beta
- BM Bone Marrow
- BME β-Mercaptoethanol
- BM-MSCs Bone Marrow-derived Mesenchymal Stem Cells
- BSA Bovine Serum Albumin
- CAM Cell Adhesion Molecule
- CO_2 Carbon Dioxide
- DRG Dorsal Root Ganglion
- ECM Extracellular Matrix
- FBS Fetal Bovine Serum
- FGF-2 Basic Fibroblast Growth Factor
- hDPSC human Dental Pulp Stem Cell
- HOG Human Oligodendrocyte
- HRP Horseradish Peroxidase
- HSC Hematopoietic Stem Cell
- MBP Myelin Basic Protein
- MFI Mean Fluorescence Intensity
- MSC Mesenchymal Stem Cell
- NaOH Sodium Hydroxide
- NDS Normal Donkey Serum
- NF Neurotrophic Factor
- NRG Neuregulin
- NSC Neural Stem Cell
- PBS Phosphate-Buffered Saline
- PDGFaa Platelet-Derived Growth Factor-AA
- PFA Paraformaldehyde
- PLL Poly- L-Lysine
- PNI Peripheral Nerve Injury
- PNS Peripheral Nervous System
- RA Retinoic Acid
- RT Room Temperature
- SC-hDPSC Schwann Cell-like human Dental Pulp Stem Cell
- SEM Standard Error of the Mean

Abstract

Background: Recently, a new technique was developed to align cells and collagen fibrils in a tethered collagen type I hydrogel. Cells within the gel attach to the matrix and self-align in parallel to the longitudinal axis in response to cell-generated tension. Alignment of cells and matrix is a feature commonly observed within tissues. For example, in the process of spontaneous peripheral nerve regeneration, Schwann cells organize themselves into columns to guide and support axonal repair. However, a long nerve defect requires bridging strategies to promote directed neurite outgrowth. The aforementioned technique could thus be employed to align Schwann cells within a collagen type I hydrogel, making an ideal candidate to treat large gap peripheral nerve injury. In order for this construct to be effective, a suitable source of Schwann cells is required. While the use of autologous Schwann cells is unfavourable, human dental pulp stem cells (hDPSCs) provide an easily accessible cell source. Furthermore, the differentiation potential of hDPSCs towards Schwann cell-like cells (SC-hDPSCs) has been described and both hDPSCs and SC-hDPSCs have been shown to contract and align within a collagen type I hydrogel.

Objective: The aim of this study was to elucidate the mechanisms by which these cells contract and interact with their matrix.

Materials and methods: Isolated hDPSCs were brought into culture and differentiated into SC-hDPSCs by exposure to specific growth factors. At first, the ability of these cells to contract within a collagen type I hydrogel was evaluated. Consequently, immunocytochemical and western blot analysis were performed to determine the expression levels of collagen type I-binding receptors. Finally, hDPSCs and SC-hDPSCs were exposed to specific inhibitors to give insight into the contribution of specific receptors in the contraction process.

Results: SC-hDPSCs showed a larger contractile ability within a collagen type I hydrogel compared to hDPSCs. Subsequent protein analysis revealed significantly higher expression of the collagen-binding receptor subunit integrin beta (β) 1 in SC-hDPSCs. Furthermore, the expression of the integrin alpha (α) 11 subunit was also increased (~2 fold), although not significant. Finally, hydrogel contraction was almost completely inhibited when the cells were exposed to an integrin β1 blocking antibody.

Discussion: Taken together, these results indicate an important role for integrin β1 in the contraction of a collagen type I hydrogel by (SC-) hDPSCs. However, given the heterodimeric nature of integrin receptors, the contribution of specific integrin alpha subunits (e.g. α11) should be explored to reveal the differential contraction potential between hDPSCs and SC-hDPSCs. These results are of high value in the development of self-aligned cellular hydrogels as a neuroregenerative therapy.

Samenvatting

Introductie: Een nieuwe techniek werd onlangs ontwikkeld om cellen en collageen vezels te aligneren in een collageen type I hydrogel, bevestigd aan beide uiteindes. Cellen binnen de gel hechten zich vast aan de collageen matrix en aligneren spontaan, parallel volgens de lengteas, in reactie op cel-gegenereerde spanning. Alignatie van cellen en matrix is een eigenschap hetgeen frequent wordt geoberveerd in weefsels. Bijvoorbeeld, gedurende het proces van spontane perifere zenuw regeneratie ordenen Schwann cellen henzelf in kolommen om zo het axonale herstel te begeleiden en ondersteunen. Echter, in het geval van ernstige zenuwschade is er een overbrugging vereist om gerichte neuriet uitgroei te stimuleren. Bovengenoemde techniek zou zodoende toegepast kunnen worden om Schwann cellen te aligneren in een collageen type I hydrogel, wat deze uitermate adequaat zou maken in de behandeling van perifere zenuwschade. Een geschikte bron van Schwann cellen is echter vereist opdat de toepassing van dit construct efficiënt zou zijn. Hoewel het gebruik van autologe Schwann cellen ongustig is, voorzien humane dentale pulpastamcellen (hDPSCs) een toegankelijke bron van cellen. Bovendien, het potentieel van hDPSCs om te differentiëren in Schwann-achtige cellen (SC-hDPSCs) is reeds beschreven en zowel hDPSCs als SC-hDPSCs bleken alvast in staat te zijn tot het contraheren van- en aligneren in een collageen type I hydrogel.

Doelstelling: Het doel van deze studie was om de mechanismen te belichten betrokken in de interactie en contractie van deze cellen met hun matrix.

Materiaal en methoden: Geïsoleerde hDPSCs werden in cultuur gebracht en gedifferentieerd in SC-hDPSCs door de blootstelling aan specifieke groeifactoren. Initieel werd het vermogen van deze cellen om een collagen type I hydrogel te contraheren onderzocht. Vervolgens, immunocytochemische en western blot analyse werd uitgevoerd om het expressie niveau te bepalen van collagen type I-bindende receptoren. Tenslotte, hDPSCs en SC-hDPSCs werden blootgesteld aan specifieke inhibitoren om inzicht te krijgen in the bijdrage van specifieke receptoren in het contractie proces.

Resultaten: SC-hDPSCs vertoonden een beter contraherend vermogen in een collageen type I hydrogel, in vergelijking met hDPSCs. De eropvolgende proteïne analyse onthulde een significant hogere expressie van de collageen-bindende receptor subeenheid integrine beta (β) 1 in SC-hDPSCs. Daarenboven, de expressie van de integrine alfa (α) 11 subeenheid was ook verhoogd (~2 maal), echter niet significant. Ten slotte, contractie van de hydrogel was bijna volledig afgeremd wanneer de cellen werden blootgesteld aan een blokkerend antilichaam gericht tegen integrine β1.

Discussie: In conclusie, deze resultaten indiceren een belangrijke rol voor integrine β1 in de contractie van een collageen type I hydrogel door (SC-)hDPSCs. Echter, gezien de heterodimerische aard van integrine receptoren, de bijdrage van specifieke integrine alfa subeenheden (bv. α11), met betrekking tot het differentiële contractie potentieel tussen hDPSCs en SC-hDPSCs, dient verder onderzocht te worden. Deze resultaten zijn van belangrijke waarde voor de ontwikkeling van spontaan alignerende cellulaire hydrogels, als therapie in het veld van neuroregeneratie.

1. Introduction

1.1 Stem cells

One of the greatest medical advances of the 20th century was the discovery of stem cells. Stem cells differ from other types of cells in the body because of two remarkable features: self-renewal and the potency to differentiate into different cell types. This means that they are able to undergo an indefinite number of replications (self-renewal) and give rise to specialized cells (differentiation) (1-3). Four types of stem cells have been defined based on their ability to differentiate into different cell types or -lineages. 1) The earliest stem cells in ontogeny are totipotent, with the ability to develop into an entire organism (including all extraembryonic tissue). 2) Pluripotent stem cells are capable of differentiating into all types of cells and tissues originating from the three germ layers: mesoderm, endoderm and ectoderm. However, these cells cannot develop into an entire organism due to the inability to form extraembryonic tissues. 3) The third type of stem cells are the multipotent stem cells. These include postnatal or adult stem cells (ASCs) and are capable of multi-lineage differentiation (generally cells of only one germ layer). 4) Finally, there are cells which can only differentiate into one defined cell type, termed unipotent or progenitor stem cells (3, 4).

1.2 Stem cells in tissue engineering

1.2.1 Adult stem cells

In recent years, numerous studies have focused on the possible application of stem cells and tissue engineering to restore the vitality and function of diseased and traumatized tissue (5, 6). Impeded by ethical concerns regarding the use of totipotent/pluripotent (embryonic) stem cells, ASCs seem to be more applicable for stem cell-mediated therapies and tissue engineering applications (2). Furthermore, ASCs retain the ability to differentiate into different cell types (commonly restricted to certain lineages), with some plasticity to transdifferentiate to cells from another germ layer (7). The primary role of ASCs is to maintain and repair the tissue of origin. Based on their presence within the body, ASCs can be subdivided into three major classes: neural stem cells (NSCs), hematopoietic stem cells (HSCs) and mesenchymal stem cells (MSCs) (1, 7).

1.2.2 Tissue engineering

Tissue engineering is a multidisciplinary field that incorporates biology, engineering and clinical science in order to mend and regenerate body structures. It involves different steps, such as the identification of appropriate cells and the development of scaffolds (2, 8). An ideal scaffold should have specific chemical and physical characteristics, so as to mimic the *in vivo* situation. The main properties are biocompatibility (to optimize tissue regeneration and reduce side effects from the immune response); biodegradability; and also specific mechanical properties (in order to be stable and endure *in vivo* stresses) (2). A common feature of biological tissues is cellular and extracellular matrix (ECM) alignment, as observed in the musculoskeletal system and some parts of the nervous

system. This organized architecture can be critical to function, and failure to recreate the aligned tissue structures is a limitation in clinical repair, with scarring and poor restoration of mechanical function being common (9-11). For this reason, much research has focused on engineering aligned cellular structures *in vitro* to regenerate structured and functional tissue equivalents (10, 11).

1.3 Peripheral nervous system

One tissue where the use of such an aligned substrate would be of great benefit for clinical repair is peripheral nerve. As mentioned before, cellular and ECM alignment actually exist within the nervous system, particularly in case of peripheral nerve regeneration (9, 11). In general, the peripheral nervous system (PNS) consists of neurons whose cell bodies are located in the spinal cord or within spinal ganglia, and their axons, which extend through peripheral nerves to reach target organs (12). Nerve fibres are grouped in fascicles in the peripheral nerve, eventually giving rise to branches that innervate specific targets. In addition, peripheral nerves are composed of three connective tissue sheaths that support and protect the complex: epineurium, perineurium and endoneurium. The epineurium is the outermost layer comprised of loose connective tissue and blood vessels to supply the nerve. It envelops the nerve and has extensions that encompass the fascicles. Furthermore, each fascicle is enclosed by a ring of dense perineurium, which consists of an inner layer of perineurial cells and an outer layer of organized collagen fibres. The innermost sheath is the endoneurium. It is composed of loose vascular connective tissue (primarily collagen type I), fibroblasts and extracellular fluid, occupying the space between the nerve fibres within the fascicle. Inside these endoneurial tubules, axons are accompanied by Schwann cells, which either myelinate or just surround the axon (12, 13).

1.3.1 Schwann cells

Schwann cells are the ensheathing glial cells of the PNS and are crucial for normal nerve function. Two types of Schwann cells can be distinguished in adult peripheral nerve: myelinating and non-myelinating (ensheathing) Schwann cells. Myelinating Schwann cells form a multi-layered myelin sheath around large-diameter axons. Unlike oligodendrocytes, the myelinating cells of the central nervous system, Schwann cells associate with just one segment of a single axon and are evenly spaced along the length of the axon. The resulting myelin structures provide insulation that allows for rapid saltatory conduction. In contrast, non-myelinating Schwann cells (or Remak cells) loosely ensheath and support small diameter sensory axons. However, in addition to their ability to form myelin (and provide trophic support), Schwann cells (both Remak and myelinating Schwann cells) have striking regenerative properties, allowing for functional repair of the PNS following injury (14, 15).

1.3.2 Peripheral nerve regeneration

In contrast to the central nervous system, the peripheral nervous system (PNS) possesses an intricate ability for repair and regeneration, in which Schwann cells play an important role. Following peripheral nerve injury (PNI), Schwann cells lose their differentiated morphology, stop producing

myelin proteins and re-enter the cell cycle. Accordingly, they upregulate genes implicated in promoting neuronal survival and axon growth (neurotrophic factors), macrophage invasion (cytokines) and activate mechanisms to break down their myelin sheaths. Furthermore, Schwann cells transform morphologically into cells with long parallel processes, forming the bands of Büngner within their endoneurial tubes. The aligned Schwann cells and their ECM (consisting primarily of collagen type I) provide indispensable tracks for guided axonal regrowth. This response allows for optimal regeneration from the proximal to the distal end of the injury. To complete the repair process, Schwann cells eventually transform again into the native myelinating cells required to envelop the regenerated axons and allow for functional recovery (11, 14, 16, 17). Neuronal regeneration and functional recovery, however, is limited by the distance between the nerve stumps and where there is a large nerve gap (>1-2 cm), bridging strategies are required to promote directed neurite outgrowth. The current clinical gold standard treatment involves the use of a nerve autograft. While providing both aligned Schwann cells and the appropriate architecture for regeneration, there are problems with availability and donor site morbidity (9, 17). Inspired by autologous nerve grafts mimicking the endogenous repair process of peripheral nerves, many studies currently focus on the exploitation of Schwann cell alignment in biomaterials towards constructing an aligned tissue-like cellular construct for neural tissue engineering (11).

1.3.3 Engineered neural tissue for peripheral nerve regeneration

Promising recent approaches to generate aligned cellular scaffolds to support nerve regeneration include, among others, the use of Schwann cell-seeded aligned fibres made from synthetic polymers (18) and seeding of Schwann cells within longitudinally cross linked collagen scaffolds (19). In all these cases a pre-aligned scaffold was used to confer alignment upon these cells. Recently a new technique was developed which resulted in the self-alignment of Schwann cells seeded within a tethered collagen type I hydrogel (20). The cells and matrix effectively organize each other into an orientated aligned structure through integrin-mediated interactions. The resulting cytoskeletal contraction of the Schwann cells applies strain to the local 3-dimensional (3D) environment, causing cells and collagen fibrils to become aligned in response to the cell-generated tension that develops longitudinally in the tethered collagen type I hydrogel (9, 10). This approach allows to engineer aligned cellular biomaterials that mimic key features of the native environment for optimal nerve regeneration. Additionally, it avoids the limitations of a cell-seeding step into a preformed scaffold (e.g. undesirable spatial and mechanical cues) (9).

1.4 Dental pulp stem cells as an alternative source of Schwann cells

In order for the aforementioned approach to be useful in a clinical setting, a suitable source of Schwann cells is required. The use of autologous Schwann cells is unfavourable due to donor site morbidity, and they are known to expand slowly *in vitro*. More importantly however, primary Schwann cells hardly contract within a collagen type I hydrogel (17). As mentioned previously, it is this intimate coupling of cell and matrix which is responsible for the self-alignment of Schwann cells and collagen fibrils (10, 17). In search of alternative cell sources, ASCs - such as MSCs - have shown to be promising candidates.

1.4.1 Mesenchymal stem cells

MSCs were firstly described as plastic-adherent cells isolated from bone marrow (BM), which possess self-renewal capacity and multipotent differentiation potential *in vitro* (21). However, MSCs are found to be present in the stroma of almost every adult organ in the human body, including adipose tissue, the umbilical cord, skeletal muscle and teeth (22-25). A panel of different cell surface antigens is used to identify MSCs in a cell population. The cells should express the following markers: CD29, CD44, CD73, CD105, CD90 and the extracellular matrix proteins vimentin, laminin and fibronectin. Furthermore, MSCs should lack expression of CD11b, CD14, CD34, CD45, CD79α and HLA-DR (1). It has been shown that MSCs can transdifferentiate towards cells of the neural lineage, yielding great potential for stem cell-based therapies and (neural) tissue engineering (26-29).

1.4.2 Human dental pulp stem cells

Gronthos *et al*. (22) were the first to isolate and characterize a population of mesenchymal-like stem cells from dental pulp tissue, labelled human dental pulp stem cells (hDPSCs). hDPSCs are ectoderm-derived stem cells, originating from migrating neural crest cells. They are described as a highly proliferative cell population possessing the self-renewal ability and multi-lineage differentiation potential. In addition, hDPSCs display MSC-characteristics such as adherence to a plastic surface, a fibroblast-like morphology, and the ability to form colonies when cultured *in vitro* (1, 2, 22). They can be easily isolated from discarded wisdom teeth - as opposed to the need for invasive tissue harvest associated with other sources of MSCs - with few ethical issues (discarded wisdom teeth are considered to be medical waste) (2, 17). Furthermore, results indicated that hDPSCs have the potential to differentiate along the neural lineage *in vitro* (1, 30). Recently, Martens *et al*. (17) reported for the first time the transdifferentiation potential of hDPSCs towards Schwann-like cells (SC-hDPSCs). SC-hDPSCs were able to promote neuronal survival and guide neurite outgrowth. Preliminary results also indicated the ability of hDPSCs and SC-hDPSCs to contract and align within a collagen type I hydrogel. Based on the multi-lineage (trans)differentiation potential of hDPSCs, their ease of isolation and the ability to contract within a collagen type I hydrogel, hDPSCs prove to be a promising stem cell population in regard to constructing an aligned tissue-like cellular construct for peripheral nerve regeneration.

1.5 Integrin receptors

As mentioned earlier (section 1.3.3), alignment of collagen fibrils and the orientation of the cells occurs through integrin-mediated interactions and cytoskeletal contraction (10). The integrins are a large family or receptors and the principal class of cell adhesion molecules (CAMs) that mediate cell-matrix interactions. An individual integrin receptor is comprised of two non-covalently bound heterodimers - alpha (α) and beta (β) subunit. Mammals contain 18 α and 8 β integrin subunits that combined can produce at least 24 different heterodimers, each of which can bind to a specific set of cell-surface-, ECM- or soluble protein-ligands. Integrins are versatile receptors. Not only do the integrin subunits collaborate in inside-out signalling which leads to the activation of the receptor, but integrins are also subjected to outside-in signalling in which the ligand-bound receptor initiates

intracellular signalling pathways. Many cellular processes like cell attachment, motility, proliferation as well as contraction are affected through this dialog (27, 31, 32). Once integrins are bound to their respective ligands, they move laterally in the plain of the membrane to form so called focal adhesion sites (clusters of integrin receptors). These specialized structures assure substrate adhesion as well as targeted localization of actin filaments and intracellular signalling components, and hence control cellular behaviour (27, 32).

1.5.1 Classification of integrins

Integrin receptors can be classified according to their preferable ECM components. Integrins α1β1, α2β1, α10β1 and α11β1 represent the primary collagen receptors; integrins α3β1, α6β1, α6β4 and α7β1 are the major laminin receptors; and integrins α5β1, α8β1, αIIbβ3 and the αvβ(3, 5, 6 and 8) integrins are the major fibronectin receptors. There also exist a number of leukocyte-specific integrin receptors, which comprise αLβ2, αMβ2, αXβ2, αDβ2 and αEβ7. However, this integrin classification is not absolute as redundancy exists with respect to certain integrin-ECM interactions. Some integrins bind the same extracellular ligands (albeit at different affinities) and conversely, some ligands are recognized by different integrins (27, 32).

1.6 Research aim and experimental setup

The aim of this study was to elucidate the mechanisms by which these cells contract and interact with their matrix. Therefore, isolated hDPSCs were brought into culture and differentiated into SC-hDPSCs by exposure to specific growth factors. At first, the ability of these cells to contract within a collagen type I hydrogel was evaluated. Consequently, immunocytochemical and western blot analysis were performed to determine the expression levels of collagen type I-binding receptors. Finally, hDPSCs and SC-hDPSCs were exposed to specific inhibitors to give insight into the contribution of specific receptors in the contraction process. As mentioned earlier, the principal class of CAMs that mediate cell-matrix interaction are the integrin receptors. Depending upon their preferable ECM ligand, integrins can be classified as fibronectin-, laminin- and collagen-binding-, and leukocyte-specific receptors. Considering the fact that hDPSCs and SC-hDPSCs will be seeded within a collagen type I hydrogel, possible candidates were narrowed down to integrins classified as collagen type I binding receptors (α1β1, α2β1, α10β1 and α11β1). Based on previous research conducted in hMSCs regarding the expression of collagen type I binding integrins (27, 33-35), the following integrin receptors were selected as the focus of our research: α1β1, α2β1 and α11β1.

2. Materials and methods

All products were purchased from Sigma-Aldrich (Bornem, Belgium) unless mentioned otherwise.

2.1 Cell culture

Human dental pulp stem cells (hDPSCs) were cultured in minimal essential medium, alpha modification (α-MEM) supplemented with 10% fetal bovine serum (FBS, Biochrom AG, Berlin, Germany), 2 mM L-glutamine, 100 U/ml penicillin, and 100 µg/ml streptomycin (further referred as standard culture medium). Cells were grown at 37 °C in a humidified atmosphere with 5% carbon dioxide (CO_2). For the purpose of optimization experiments, the human oligodendroglial cell line (HOG) was maintained in RPMI medium 1640 + Glutamax™ (Gibco®, Paisley, Scotland) supplemented with 10% FBS, 100 U/ml penicillin, and 100 µg/ml streptomycin. HOGs were incubated at 37°C in a humidified atmosphere with 10% CO_2. In general, the culture medium was changed every 2-3 days. After reaching 80-90% confluence, cells were trypsinized using 0.05% Trypsin-EDTA (0.5 g/l porcine trypsin and 0.2 g/l EDTA), for 5 minutes at 37 °C, and subcultured at a density of 3.2 x 10^3 cells/cm^2.

2.1.1 Differentiation of hDPSCs into Schwann-like cells

In order to subject hDPSCs to Schwann cell differentiation, cells at passage 1-2 were seeded at a density of 2.6 x 10^3 cells/cm^2. Prior to seeding, culture flasks were coated through incubation with 10 µg/ml poly-L-lysine (PLL) for 1 hour at room temperature (RT), followed by a washing step with MilliQ. After 3 days, differentiation was induced by switching the medium to standard culture medium without FBS containing 1 mM β-mercaptoethanol (BME) for 24 h. Subsequently cells were incubated in standard culture medium supplemented with 35 ng/ml retinoic acid (RA). In between medium changes, cells were rinsed with phosphate-buffered saline (PBS) (pH 7.4). After 72 h, the medium was replaced by standard culture medium containing 5 µM forskolin, 10 ng/ml basic fibroblast growth factor (FGF-2), 5 ng/ml platelet-derived growth factor-AA (PDGFaa) and 200 ng/ml heregulin-β1 (neuregulin, NRG) (Immunotools, Friesoythe, Germany). Cells were cultured in this differentiation medium for another 14 days (37 °C and 5% CO_2 in humidified air) with medium changes every 2-3 days. hDPSCs differentiated toward Schwann-like cells are henceforward referred to as SC-hDPSCs.

2.1.2 Isolation of primary Schwann cells

Experimental procedures involving neonatal animals were approved by the Hasselt University animal ethics advisory group. For the isolation of primary Schwann cells, five-day-old Sprague-Dawley rat pups (P5) were sacrificed by decapitation. Accordingly, sciatic nerves were exposed, dissected out and placed in L15 medium on ice. Following isolation, the nerves were carefully stripped free of epineurium and collected in fresh L15 medium. The nerve segments were enzymatically dissociated using 125 µl medium, consisting of 0.25% collagenase in DMEM/F12 medium (Gibco®, Paisley, Scotland) without FBS, per nerve segment at 37 °C for 45 min. Subsequently the collagenase solution

was removed and nerve segments were incubated with 0.25% trypsin (Gibco®, New York, USA) diluted in 1x PBS for 5 min at 37 °C. After enzymatic digestion, the sciatic nerve segments were mechanically dissociated until a homogeneous suspension was obtained. The cell suspension was pelleted at 178 g for 5 min, using an Eppendorf 5804R centrifuge (Eppendorf AG, Hamburg, Germany), and resuspended in DMEM/F12 supplemented with 10% FBS, 100 U/ml penicillin, and 100 µg/ml streptomycin (further referred as DMEM/F12 complete medium). Cells from 8-10 nerve segments were seeded in a T75 culture flask precoated with 10 µg/ml PLL (as described in section 2.1.1). The next day, cultured cells were incubated in DMEM/F12 complete medium with 10 µM cytosine arabinoside (Ara-C) for 24 h. Following two wash steps with serum-free medium, DMEM/F12 complete medium supplemented with 20 ng/ml NRG was added. After another 48 h in culture, cells were treated with 0.05% trypsin (diluted in 1x PBS) at RT. While gently shaking the culture flask, cells were continuously monitored under the light microscope until the majority of the Schwann cells were loose. This step takes advantage of the differential cell detachment between Schwann cells and fibroblasts in a process called selective trypsinisation. The resulting cell suspension was then pelleted and subcultured in DMEM/F12 complete medium with 20 ng/ml NRG. These latter steps were performed to purify the Schwann cell culture from contamination by fibroblasts.

2.1.3 Isolation of dorsal root ganglions (DRGs)

Experimental procedures involving adult animals were approved by the Hasselt University animal ethics advisory group. Adult Sprague-Dawley rats were sacrificed, after which the spinal column was removed. DRG explants were isolated and collected in DMEM supplemented with 10% FBS, 100 U/ml penicillin, and 100 µg/ml streptomycin (further referred as DMEM complete medium). After removal of connective tissue and sensory (afferent/efferent) nerve roots, DRGs were incubated with a 0.125% collagenase solution (diluted in DMEM containing 10% FBS) for 90 min at 37 °C. Subsequently, explants were triturated until a homogeneous suspension was obtained. Cells were pelleted at 178 g for 10 min, resuspended in DMEM complete medium with 10 µM Ara-C and seeded in a T75 culture flask (1 animal per T75 flask) precoated with 10 µg/ml PLL (as described in section 2.1.1) for 24 h.

2.2 Collagen contraction assay

Collagen contraction assays were performed to investigate the ability of hDPSCs and SC-hDPSCs to contract within a collagen type I hydrogel. Gels were prepared on ice by mixing 1 volume of 10x MEM with 8 volumes of type I rat tail collagen (2 mg/ml in 0.6% acetic acid; First Link, Wolverhampton, UK). The pH of the mixture was neutralized dropwise using 1 M sodium hydroxide (NaOH), after which 1 volume of cell suspension was added to give a final concentration of 10^6 cells/ml per gel. In this case, hDPSCs and SC-hDPSCs were trypsinized (0.5 g/l porcine trypsin and 0.2 g/l EDTA), counted and cell suspensions containing the desired number of cells were centrifuged (8 min at 258 g). The cell pellet was resuspended in either standard culture medium or differentiation medium and kept on ice until use. In order to measure contraction over time (for both hDPSCs and SC-hDPSCs), cell-seeded collagen hydrogels were cast in a 96-well plate (Greiner F-bottom; 75 µl/well) for five different time points (2, 4, 6, 8 and 24 hours in duplo). After 15 min of polymerization at 37 °C, gels were immersed in 200 µl medium (standard culture or differentiation medium) and

manually detached from the wells using a needle. Hydrogel contraction was monitored by digital images taken at indicated time points. Images were imported into ImageJ and contraction was measured as a percentage of the initial hydrogel surface (1-(area contracted hydrogel/area well) * 100). For each time point, the average of the replicates was measured and further processed into a graph depicting the hydrogel contraction profile.

2.3 Myelination in collagen hydrogel

In order to investigate the myelination potential of hDPSCs and SC-hDPSCs within a 3D environment, cells were seeded together with DRG neurons in a collagen type I hydrogel. Gels were prepared as described in section 2.2 with some slight modifications. In order to allow for long-term incubation a higher concentration of type I rat tail collagen (5 mg/ml in 0.6% acetic acid; First Link, Wolverhampton, UK) was applied to the mixture. Furthermore, the cell suspension was prepared using 250,000 hDPSCs or SC-hDPSCs and 5 dissociated DRG bodies per ml of gel. DRG neurons were harvested 24 h after incubation in DMEM complete medium supplemented with 10 µM Ara-C (see section 2.1.3). The resulting cellular hydrogel mixture (1 ml) was then added to a rectangular stainless steel mold (on ice) and tethered at each end through the use of a porous mesh. The gels were allowed to set for 15 min at 37 °C and were topped afterwards with DMEM complete medium. Tethered gels were incubated for either 3 or 26 days (short and long term respectively) at 37 °C in a humidified atmosphere containing 5% CO_2 with medium changes every 2-3 days.

2.4 Immunocytochemistry

For immunocytochemical analysis, hDPSCs and SC-hDPSCs were seeded on 12 mm glass coverslips (PLL coated for SC-hDPSCs) at a concentration of 2 x 10^4 cells in standard culture medium or differentiation medium respectively. When cells reached 70-80% confluency, they were fixed in 4% paraformaldehyde (PFA) for 20 min at RT and subsequently rinsed two times in 1x PBS. When the target epitope of the primary antibody was located intracellularly (as was the case for integrin α1), cells were permeabilized with 0.05% Triton X-100 in 1x PBS for 30 min at 4 °C. Aspecific binding sites were blocked by incubating cells with 10% normal donkey serum (NDS) (Millipore, MA, USA) in 1x PBS for 30 min at RT. After washing with 1x PBS, cells were incubated with the primary antibodies, listed in table 1, for either 1 h at RT or overnight at 4 °C. Samples in which the primary antibody was omitted were used as a blanco. Prior to adding the secondary antibody, cells were washed four times with 1x PBS. Depending on the primary antibody, cells were incubated with either donkey anti-rabbit Alexa 488 (1/1000) or donkey anti-mouse Alexa 555 (1/1000) for 1 h at RT in the dark. Following three wash steps with 1x PBS, the 4’ ,6-diamidino-2-phenylindole (DAPI) nuclear counterstain was performed for 10 min at RT (in the dark). Coverslips were mounted with Dako fluorescent mounting medium (Dako, Heverlee, Belgium) on glass slides (Thermo-Scientific; Menzel-Gläser, Braunschweig, Germany). Samples were evaluated using a Nikon Eclipse 80i fluorescence microscope equipped with a Nikon DS-2MBWc digital camera (Nikon, Tokyo, Japan). Quantification of the fluorescent images was performed using ImageJ, by measuring the mean fluorescence intensity (MFI) per cell. Fluorescent images of hDPSCs were used to establish the reference settings in ImageJ (upper and lower threshold) in order to measure the MFI/cell of both hDPSCs and SC-

hDPSCs for each staining. This allowed to calculate the relative difference in protein expression of SC-hDPSCs compared to hDPSCs.

Table 1. Overview of the primary antibodies used for immunocytochemical analysis.

Primary antibody	Species	Dilution	Manufacturer
Integrin α1	Rabbit polyclonal	1/200	Abcam (ab78479)
Integrin α2	Mouse monoclonal	1/100	Abcam (ab55340)
Integrin β1	Mouse monoclonal	1/100	Abcam (P5D2)

2.5 Western blot

2.5.1 Optimization for the detection of myelin proteins

To investigate the myelination potential of hDPSCs and SC-hDPSCs, western blot was optimized for the detection of myelin proteins. HOGs – known to produce abundant myelin proteins – were processed as a number of different samples to be used in the western blot. HOGs were either simply pelleted from 2D cultures or seeded within a collagen type I hydrogel (as described in section 2.2) and cast in a rectangular stainless steel mold tethered at each end. Furthermore, to determine the optimal method for harvesting such cell-seeded collagen type I hydrogels, samples were either crushed in liquid nitrogen or degraded through collagenase. In the latter case, the gel was cut from the mold, transferred to a 24-well plate, washed briefly with 1x PBS and incubated with 0.2% collagenase (diluted in medium without FBS) for 1 h at 37 °C. When the gel was completely digested (no mechanic dissociation), the supernatant was collected in an eppendorf and adherent cells in the 24-well plate were trypsinized (0.5 g/l porcine trypsin and 0.2 g/l EDTA) and collected in the same eppendorf. The cell suspension was then pelleted at 2000 rpm for 10 min. To reduce collagen debris, the resulting pellet was washed with PBS and centrifuged again and this procedure was repeated 2 more times). In general, for protein extraction, samples were lysed in ice cold RIPA buffer (from Abcam: "Western blotting - a beginners guide") supplemented with complete protease inhibitor cocktail (1/4 tablet for 2.5 ml) (Roche Diagnostics, Basel, Switzerland). The cell pellet yielded from a collagen hydrogel, for the detection of myelin proteins, was generally lysed in 50 µl of RIPA buffer. Following sonication, 20 pulses of one second using a needle sonicator, samples were centrifuged at 3000 g at 4 °C for 20 min in order to discard large nuclear debris. The resulting supernatant was stored at -80 °C. The protein concentration was determined by using the bicinchoninic acid (BCA) protein assay kit (Thermo Scientific, IL, USA) following standard protocol. The measurements were performed at 540 nm by means of the FLUOstar Optima microplate reader (BMG Labtech, Ortenberg, Germany).

SDS-PAGE was performed according to a standard protocol. Briefly, 10 µg of protein samples were loaded on 12% polyacrylamide gels, under denaturing and reducing conditions (without heating of the samples). Electrophoresis initially was run at 100V until the samples reached the separating gel, after which the voltage was increased to 150V to complete the run. Subsequently proteins were transferred onto a PVDF membrane for 90 min at 350 mA. The membrane was incubated with

blocking solution consisting of 5% bovine serum albumin (BSA) in PBS for 1 h at room temperature with gentle shaking. Afterwards the membrane was incubated with the primary antibody diluted in 2% BSA, overnight at 4° C. After washing with 0.05% PBS-Tween20, the membrane was incubated with a horseradish peroxidase (HRP) labeled secondary antibody for 1 h at room temperature. The membrane was washed 3x5 min in 0.05% PBS-Tween and 30 min in MilliQ to reduce background signals. Finally, the membrane was incubated with Pierce ECL plus western blotting substrate for 5 min at room temperature in the dark, followed by chemiluminescent detection using an Image Quant LAS 4000 mini. In general, beta-actin (mouse monoclonal; 1:5000; Santa Cruz, Heidelberg, Germany) was used for normalization in processing of the results.

2.5.2 Detection of myelin proteins in collagen hydrogel

After optimization for the detection of myelin proteins, the samples described in section 2.3 were used in western blot. Processing of the collagen hydrogel - through incubation with 0.2% collagenase - and protein extraction was executed as described previously. SDS-PAGE and subsequent protein detection was performed as mentioned in section 2.5.1, with some small modifications. The primary antibody used was directed against myelin basic protein (anti-MBP, rabbit polyclonal, Santa Cruz (FL-304)) at a 1:250 dilution. Afterwards the membrane was incubated with a HRP labeled secondary goat α rabbit antibody (1:5000). The rest of the protocol was performed as described in section 2.5.1

2.5.3 Integrin detection

In order to quantify integrin expression levels of hDPSCs and SC-hDPSCs western blot analysis was performed. 2D cultures of hDPSCs and SC-hDPSCs were used to prepare cell lysates for western blot, according to the following protocol. Initially, cells were washed with ice-cold PBS and after draining the PBS, ice-cold lysis buffer was added (1 ml per 10^7 cells). Subsequently, adherent cells were scraped of the culture flask using a cold plastic cell scraper and the resulting cell suspension was transferred into a pre-cooled microfuge tube. Following constant agitation for 30 min at 4 °C, the cell suspension was centrifuged for 20 min at 12000 rpm. The supernatant was aspirated and placed in a fresh eppendorf and afterwards stored at -80 °C. SDS-PAGE was performed according to standard protocol (view section 2.5.1), with some slight modifications. Briefly, 5 µg of protein sample was loaded on 7.5% polyacrylamide gels under denaturing conditions (no BME). Furthermore, samples were heated for 10 min at 70 °C prior to loading. Primary and secondary antibodies used are listed in table 2.

Table 2. List of primary and secondary antibodies used in the detection of integrins.

Primary antibody	**Species**	**Dilution**	**Manufacturer**	**Secondary antibody**	**Dilution**
Integrin α1	Rabbit polyclonal	1/1250	Abcam (ab78479)	Goat α rabbit	1:5000
Integrin α11	Rat monoclonal	1/1000	R&D systems	Rabbit α mouse	1:5000
Integrin β1	Mouse monoclonal	1/100	Abcam (P5D2)	Rabbit α rat	1:5000

2.6 Inhibition hydrogel contraction

In order to determine the contribution of certain collagen type I-binding integrin subunits in the contraction process of both hDPSCs and SC-hDPSCs, an inhibition experiments was set up. Cell-seeded collagen hydrogels were prepared as described in section 2.2. In this case however cell suspensions, of hDPSCs and SC-hDPSCs, were prepared for a number of different conditions (trypsinization, cell counting and pelleting). After removal of the supernatant, cell pellets were resuspended in medium (standard culture medium or differentiation medium) containing different concentrations of blocking antibodies (anti-integrin α1 (ab33410) or anti-integrin β1 (ab24693); Abcam) (10 µg/ml, 1 µg/ml, 0.1 µg/ml and 0.01 µg/ml). Furthermore, a negative control (either an IgG2a or IgG1 isotype control at 10 µg/ml) and a blanco (blocking antibody omitted) were incorporated. Cell pellets were allowed to incubate in blocking or 'control' medium for 20 min, on ice, after which the right amount of neutralized collagen suspension was added (attaining a final concentration of 10^6 cells/ml). For each condition, hDPSCs and SC-hDPSCs, 75 µl of this cellular collagen solution was pipetted in a 96-well plate (Greiner, F-bottom) in duplo. After polymerization, 150 µl medium (standard or differentiation) containing the appropriate concentration of antibody was added to the corresponding wells. The hydrogels were detached from the wells using a needle and allowed to incubate for 8 h at 37 °C. After 8 h, digital images were taken from the hydrogels. Images were imported into ImageJ and contraction was measured as a percentage of the initial hydrogel surface (as described in section 2.2).

2.7 Statistical analysis

Statistical analysis was performed using GraphPad Prism 5 software (GraphPad, San Diego, CA, USA). Data from the hydrogel contraction profile were compared between hDPSCs and SC-hDPSCs by means of a 2-way ANOVA (repeated measures) followed by Bonferroni's multiple comparison test. Data from immunocytochemistry and western blot analysis were compared by means of a Mann-Whitney test. Data were represented as mean ± standard error of the mean (SEM). P-values ≤ 0.05 were considered statistically significant.

3. Results

3.1 Morphological differentiation of hDPSCs towards Schwann-like cells

hDPSCs at passage 1-2 were subjected to Schwann cell differentiation. Following the induction protocol, cells changed from a flattened fibroblast-like morphology (**Fig. 1A**) to an elongated bipolar cell shape (**Fig. 1B**), resembling primary rat Schwann cells in culture (**Fig. 1C**).

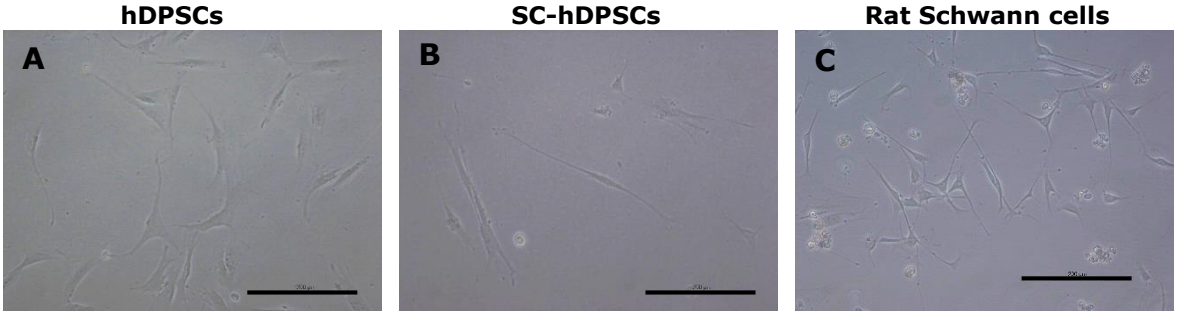

Figure 1. Morphological analysis of hDPSCs after Schwann cell differentiation. Brightfield images of hDPSCs (A), SC-hDPSCs (B), and primary rat Schwann cells (C). Scale bars = 200 µm.

3.2 SC-hDPSCs display a faster contractile ability within a collagen type I hydrogel compared to hDPSCs

The ability of hDPSCs and SC-hDPSCs to contract within a collagen type I hydrogel was assessed through collagen contraction assays. At five different time points (2, 4, 6, 8 and 24 h) contraction was captured for both hDPSCs and SC-hDPSCs and measured as a percentage of the initial surface area of the hydrogel (**Fig. 2**). While contraction was similar after 2 h, SC-hDPSCs displayed a significant difference at 4 and 6 h - attaining a larger percentage of contraction - compared to hDPSCs. Eventually contraction attenuated for SC-hDPSCs after 6 h (reaching a maximum of approximately 60% after 24h). Concurrently, hDPSCs were able to approximate the percentage of contraction of SC-hDPSCs, which was already noticeable at 8 h. These results show that SC-hDPSCs are capable of realizing faster hydrogel contraction, compared to hDPSCs. In the end however, hDPSCs and SC-hDPSCs contract the collagen type I hydrogel to the same extent.

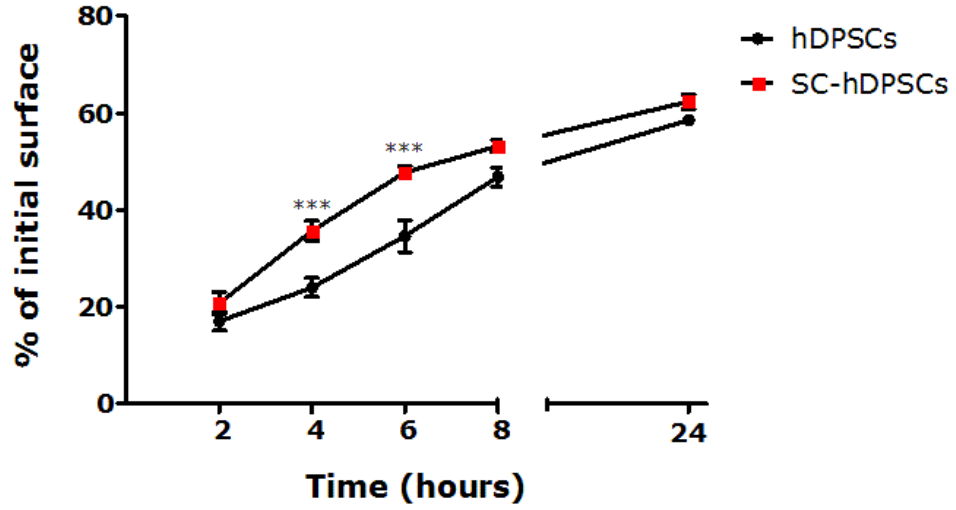

Figure 2. Hydrogel contraction profile for hDPSCs and SC-hDPSCs. SC-hDPSCs showed a significant increase in contractile ability, evident at 4 and 6 h, compared to hDPSCs. Data represent means ± SEM (n = 4). ***P < 0.001.

3.3 Immunocytochemical characterisation of integrin α1, α2 and β1 expression by hDPSCs and SC-hDPSCs

Previously observed distinction in contractile ability between hDPSCs and SC-hDPSCs could be due to a differential expression of certain collagen type I binding integrins. Of particular interest are the following integrin receptors: α1β1, α2β1 and α11β1 (27, 33, 34). Consequently, hDPSCs and SC-hDPSCs were screened in the first place for the expression of integrin subunits α1, α2 and β1 through means of immunofluorescent stainings. Integrin α1 and β1 were found to be abundantly expressed by both hDPSCs and SC-hDPSCs (**Fig. 3A-D**), however in case of the integrin α2 subunit no signal could be detected (**Fig. 3E-F**). Furthermore, the staining for α1 and β1 subunits revealed strong focal adhesion formation (clustering of the integrin receptors at the cell membrane) in both hDPSCs and SC-hDPSCs (**Fig. 3A-D**, arrows). In order to determine potential differences in protein expression levels, quantitative analysis of the fluorescent images of hDPSCs and SC-hDPSCs (only for integrin α1 and β1 since integrin α2 expression was below detection level) was performed (**Fig. 3G**). While the expression of integrin α1 was not significantly altered in SC-hDPSCs, the expression of the integrin β1 subunit was significantly increased (approximately 2.4-fold) in SC-hDPSCs, compared to hDPSCs.

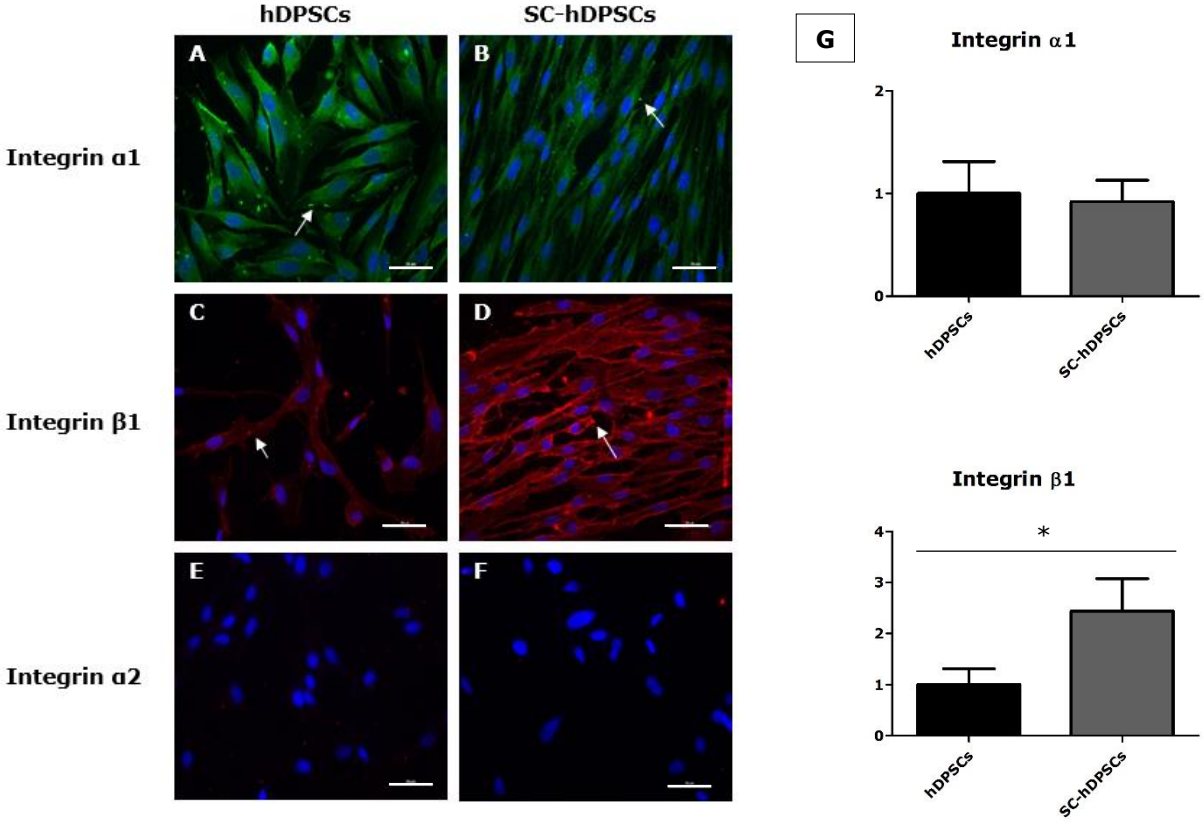

Figure 3. Expression of collagen type I binding integrins α1, α2 and β1 in hDPSCs and SC-hDPSCs. Immunocytochemistry was performed on hDPSCs (A, C, E) and SC-hDPSCs (B, D, F) for the collagen type I binding integrin subunits α1, β1 and α2. Nuclei were counterstained with DAPI (blue). Arrows indicate focal adhesion points. Protein expression levels were quantified for integrin α1 (n = 4) and β1 (n = 5) (G) and are represented as relative fold increase (compared to hDPSCs). Scale bars = 50 μm. Data represent means ± SEM. *$P < 0.05$.

3.4 Differential expression of integrin α1, α11 and β1 after differentiation

In order to confirm the results obtained by immunocytochemistry, the expression of collagen type I binding integrins in hDPSCs and SC-hDPSCs was further investigated through western blot (**Fig. 4A-B**). Similar to the results in section 3.3, a strong integrin β1 expression could be detected (two bands) in both hDPSCs and SC-hDPSCs. The upper band represents the mature, glycosylated form of the integrin β1 subunit present at the cell membrane, while the lower band corresponds to the immature form of the β1 subunit residing in the cytoplasm. Integrin α1 however produced a less pronounced signal. Furthermore the expression of the integrin α11 subunit was also investigated by western blot, which displayed an apparent band in hDPSCs prior and post differentiation. The total protein input of the samples was normalized according to the blot of beta-actin (**Fig. 4A**). Quantification of the respective blots was performed in order to determine the relative protein expression levels of hDPSCs and SC-hDPSCs (values were normalized against beta-actin) (**Fig. 4B**). In concordance with the results obtained from immunocytochemical stainings, the expression of the integrin β1 subunit was significantly increased in SC-hDPSCs (approximately 5-fold) compared to

hDPSCs. The expression of integrin α1 and α11 was slightly increased in SC-hDPSCs (approximately 1.3-fold and 1.9-fold respectively), although not significant.

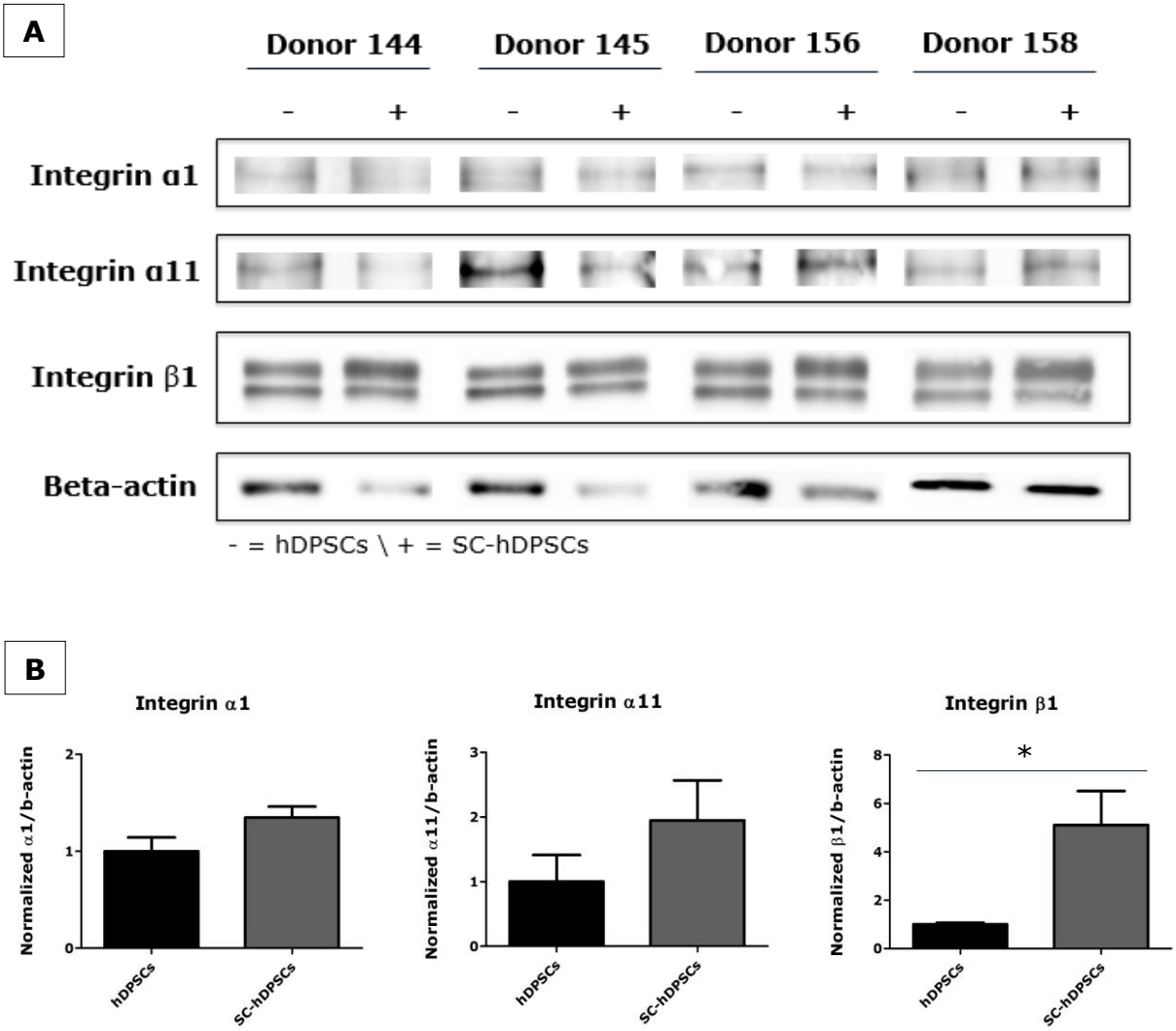

Figure 4. Differential expression of the collage type I binding integrin subunits α1, α11 and β1 after differentiation. Western blot analysis was performed to investigate protein expression levels between hDPSCs and SC-hDPSCs for four different donors (n = 4) (A). Consequent quantification was carried out to determine the protein expression levels of integrin α1, α11 and β1 in SC-hDPSCs, compared to hDPSCs (B). Values were normalized against beta-actin and are represented as relative fold increase. Data represent means ± SEM. *$P < 0.05$.

3.5 Integrin β1 plays a major role in the contraction process of hDPSCs and SC-hDPSCs in a collagen type I hydrogel

Previous experiments have shown that SC-hDPSCs possess a larger contractile ability within a collagen type I hydrogel compared to hDPSCs. Furthermore, immunocytochemical and western blot analysis revealed that the expression of the collagen type I binding integrin β1 subunit is considerably increased in SC-hDPSCs (and to a lesser extent α11 and α1). An inhibition experiment was set-up in

order to investigate the contribution of specific integrin subunits (α1 and β1) in the contraction process of collagen type I hydrogels (through antibody-based blocking). For each experiment, four different concentrations (10-1-0.1-0.01 µg/ml) of the respective blocking antibody were incorporated as well as an isotype control and a blanco. After 8 h, contraction was captured and measured (as a percentage of the initial surface area of the hydrogel). Blocking of the integrin β1 subunit markedly reduced contraction at the two highest concentrations, in both hDPSCs and SC-hDPSCs. At lower concentrations (from 0.1 µg/ml) contraction reached normal percentages, equal to those of the blanco and the negative control (**Fig. 5A**). In contrast, integrin α1 inhibition had no effect, at any concentration, on the contraction of hDPSCs and SC-hDPSCs in a collagen type I hydrogel (**Fig. 5B**).

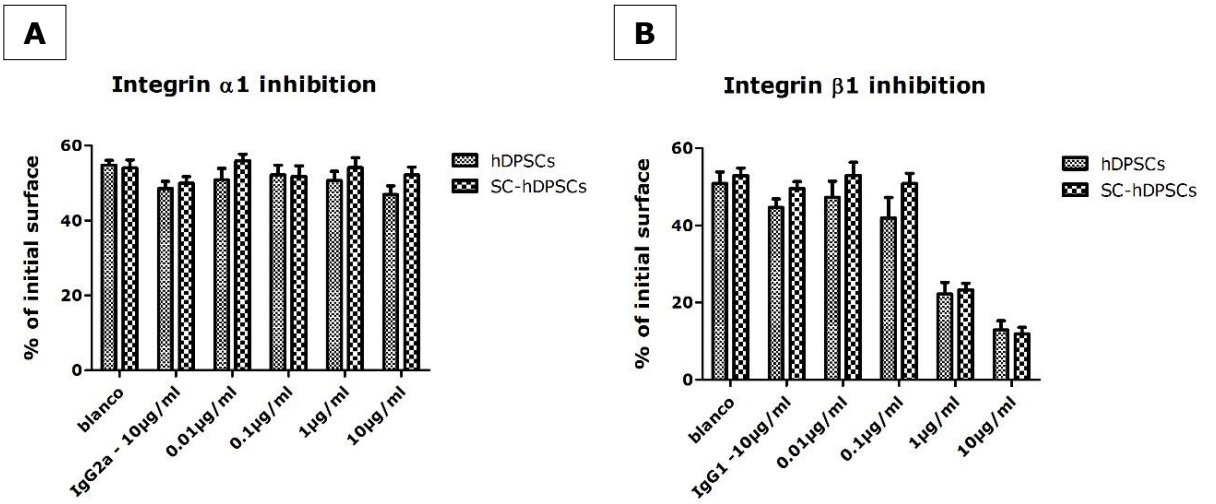

Figure 5. Inhibition of integrin subunits α1 and β1. Inhibition experiments were performed to determine the contribution of the respective subunits in the contraction process of hDPSCs and SC-hDPSCs in a collagen type I hydrogel. Data represent means ± SEM (n = 4)

3.6 Myelination potential of hDPSCs and SC-hDPSCs within a 3D environment

The main focus of this study was to elucidate the mechanisms by which hDPSCs and SC-hDPSCs contract and interact with a collagen type I matrix, as shown by the previous results. Additionally, the myelination potential of these cells was investigated.

3.6.1 Optimization for the detection of myelin proteins

In order to investigate the myelination potential of hDPSCs and SC-hDPSCs, western blot was optimized for the detection of myelin basic protein (MBP) (as described in section 2.5). Initially, the optimal method to harvest cell-seeded collagen type I hydrogels (crushed in liquid nitrogen or degraded through collagenase), to maximize the protein yield, was determined. Afterwards, the method for detecting myelin proteins (MBP) by western blot was optimized. Samples were subjected to denaturing and/or reducing conditions (with or without heating of the samples) to investigate the effect on protein configuration and subsequent migration through the polyacrylamide gels. Furthermore, different concentrations of the primary and secondary antibody were tested in order to

determine the ideal combination that gives rise to the clearest signals after chemiluminescent detection (no background, aspecific bands).

Samples which were degraded through collagenase and subjected to denaturing and reducing conditions (without heating) prior to loading delivered the best results (**Fig. 6**). Furthermore the optimal primary (anti-MBP) and secondary antibody concentrations were established to be 1:250 and 1:5000 respectively (data not shown).

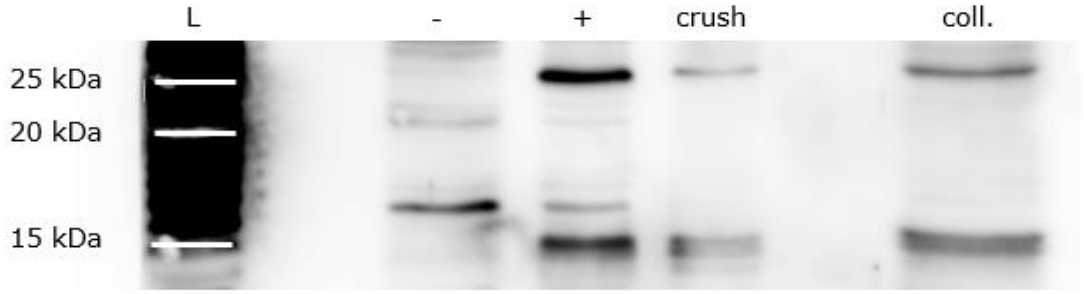

Figure 6. Representative western blot regarding optimization for the detection of MBP. Two isoforms of MBP could be detected in HOGs (at ~25 and 14kDa). Samples were loaded under denaturing and reducing conditions (no heating). The primary and secondary antibody concentrations used were 1:250 and 1:5000 respectively. Legend: L = ladder; - = negative control; + = positive control; crush = samples degraded through crushing; coll. = samples degraded with collagenase.

3.6.2 Preliminary results of myelination by hDPSCs and SC-hDPSCs in a collagen type I hydrogel.

Following optimization, samples (short & long term) described in section 2.3 were used in western blot. Briefly, hDPSCs or SC-hDPSCs were seeded together with DRG neurons in a collagen type I hydrogel and allowed to incubate for either a short period of time (3 days) or for a longer period (26 days). The total protein input of the samples was normalized to beta-actin. Two isoforms of MBP (17 and 14kDa) could be detected in both hDPSCs and SC-hDPSCs. In the short term samples exclusively the 17kDa isoform was present. However after 26 days, the protein expression levels of the 17kDa isoform had declined, while the 14kDa isoform became apparent in the samples (**Fig. 7**). This was the case for both donors.

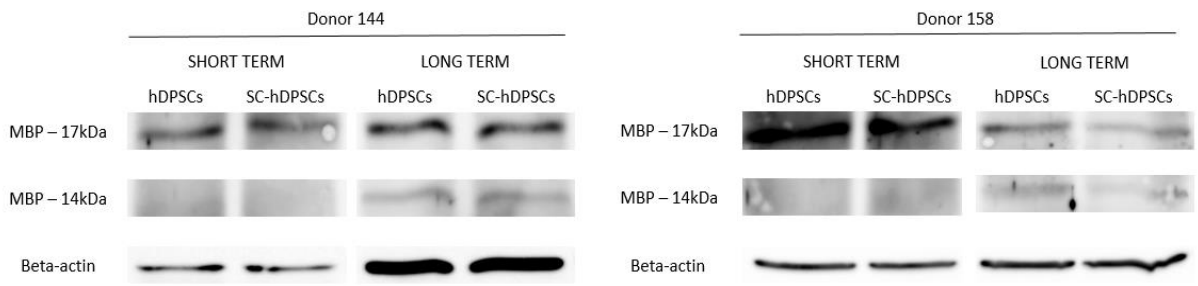

Figure 7. Myelin production by hDPSCs and SC-hDPSCs in a 3D environment. Western blot analysis was performed on short (three days in culture) and long term (26 days in culture) samples, of 2 different donors (n = 2), for the detection of myelin proteins. Two different isoforms were detected (14kDA and 17kDa), which appear to have a specific temporal distribution.

4. Discussion

In the present study, we investigated the mechanisms by which hDPSCs and SC-hDPSCs contract and interact with a collagen type I hydrogel. A number of studies already described the expression of integrin subunits on hMSCs (35-37) as well as their interaction with a collagen type I hydrogel (33). However, this is the first time that the expression of collagen type I-binding integrin receptor subunits, in hDPSCs and SC-hDPSCs, and their role in contraction has been characterized. Following the differentiation protocol, hDPSCs adopted an elongated bipolar cell morphology, resembling Schwann-like cells (further referred to as SC-hDPSCs). SC-hDPSCs realized faster contraction of a collagen type I hydrogel, compared to hDPSCs, which was accompanied by a significant increase in integrin β1 protein levels (as determined through immunocytochemistry and western blot). Furthermore, contraction was markedly impeded after antibody-based inhibition of the β1 subunit, while no effect was observed after blocking integrin α1. As an additional objective, the myelination potential of SC-hDPSCs, compared to hDPSCs, was investigated. Using a 3D coculture model with DRG neurons, preliminary western blot results indicated the expression of myelin proteins - in a timely manner - in both hDPSCs and SC-hDPSCs.

In the field of neural tissue engineering, much research has focused on the development of highly aligned cellular scaffolds. For optimal nerve regeneration across a long gap, it is essential to use a scaffold that mimics the environment during endogenous repair: Schwann cells secreting neurotrophic factors; Schwann cells organized into aligned tracts (bands of Büngner) and an aligned collagen type I extracellular matrix (11, 17). Phillips *et al.* developed a technique which resulted in the self-alignment of Schwann cells seeded within a tethered collagen type I hydrogel (20). This method exploits the natural ability of cells and ECM to form aligned 3D structures in response to cell-generated tension (due to cytoskeletal contraction). A collagen type I hydrogel, the scaffold of preference in this study, has several advantages in regard to neural tissue engineering. First of all, hydrogels made from natural proteins possess functional ECM characteristics, are biocompatible, and prove suitable as carriers for different cell types (38). Secondly, collagen type I is the most abundant ECM protein in peripheral nerves, packed around each nerve fiber to form the walls of the endoneurial tubes (12). Aforementioned aligned cellular construct (Schwann cells seeded within a collagen hydrogel) therefore incorporates key features of the peripheral nerve known to contribute to the repair process. The use of autologous Schwann cells, however, is unfavorable due to the morbidity of the donor nerve and issues with expanding the Schwann cell culture *in vitro*. More importantly in this setting, the capacity of primary Schwann cells to contract and align within a collagen type I hydrogel is limited (attaining much slower contraction) (9, 26). In search of alternative cell sources, MSCs have shown to be promising candidates. They can be isolated from a wide range of tissues, but many studies concentrated on the use of either bone marrow-derived mesenchymal stem cells (BM-MSCs) or adipose tissue-derived mesenchymal stem cells (AT-MSCs) (26, 39, 40). These stem cells comply with the criteria for ideal transplantable cells in nerve guidance scaffolds for nerve regeneration. BM-MSCs and AT-MSCs proliferate rapidly in culture and raise no major ethical issues associated with their use. More importantly, they have the ability to differentiate along neural and

corresponding glial cell lineages (26, 39-41). One major drawback, however, is the need for invasive tissue harvest (bone marrow aspiration or liposuction) with the chance of donor site morbidity.

Recently, hDPSCs have been investigated as potential alternative cell source for Schwann cells. hDPSCs have been described as MSCs from the human dental pulp, with the ability to differentiate into mesodermal and neural cell lineages (1, 22, 30, 42). They are a plastic adherent fibroblast-like cell type that can be easily isolated from the dental pulp of discarded teeth. Furthermore, DPSCs are characterized by a high proliferation capacity, plasticity and possessing immunomodulatory functions (1, 42, 43). Recently, the differentiation capacity of hDPSCs towards Schwann like cells (referred to as SC-hDPSCs) has been described. Differentiation of hDPSCs towards SC-hDPSCs was induced by the addition of a number of components: BME, RA and standard growth medium supplemented with a cocktail of growth factors (forskolin, b-FGF, PDGFaa and NRG). BME and RA - known to induce a neuronal-like phenotype – together with the further addition of aforementioned growth factors synergistically promoted the differentiation of hDPSCs towards cells with Schwann-like characteristics (44, 45). This makes SC-hDPSCs interesting candidates for neural tissue engineering and regenerative medicine. Additionally, SC-hDPSCs have proven to be more potent in producing neurotrophic factors (NFs) and promoting neurite outgrowth, compared to hDPSCs (17).

Since previous results have shown that hDPSCs are able to differentiate into SC-hDPSCs, capable of secreting NFs (17), the ability of SC-hDPSCs (compared to hDPSCs) to contract within a collagen type I hydrogel was investigated. As mentioned earlier, contraction of cells generates tension within tethered gels, required for cells and collagen fibrils to become aligned. Although both hDPSCs and SC-hDPSCs were able to contract the collagen gel, the latter were more potent (displaying faster contraction). After 6 h, contraction slowed down in SC-hDPSCs, consequently allowing hDPSCs to achieve a similar level of contraction. Ultimately, this contraction stabilized for both hDPSCs and SC-hDPSCs 24 h after casting the hydrogel, due to limitations regarding the extent to which a collagen hydrogel can contract. A number of factors can influence hydrogel contraction, possibly explaining the observed difference between hDPSCs and SC-hDPSCs. These include cell count (more cells equals faster contraction), density of the hydrogel (hydrogels with a higher collagen concentration are more difficult to contract), and cell type (46). While cell count and collagen density were the same for every condition in our experiment, there was a distinction in cell type (hDPSCs compared to SC-hDPSCs). Accordingly, different cell types can express different levels of CAMs (responsible for the intimate coupling of cell and matrix).

The principal class of CAMS that mediate cell-matrix interactions are the integrin receptors. These integrated-mediated interactions between cell and matrix activate a number of downstream processes including cytoskeletal contraction (generating the force that contracts the gel) (10, 27). As such, aforementioned difference in contractile ability could be explained by the differential expression of certain integrin receptors, between hDPSCs and SC-hDPSCs. Integrins can be classified according to their preferable ECM ligands, among them are: fibronectin, laminin, various collagens, tenascin, vitronectin and members of the SIBLINGs family (small integrin binding ligand, N-linked glycoproteins) (27). In this research we focused on the family of the collagen (type I) binding receptors, due to the nature of the scaffold used in our experiments (as described previously). In

general four integrin heterodimers (α1β1, α2β1, α10β1, and α11β1) are functioning as collagen receptors. Based on previous research performed in hMSCs regarding the expression of collagen binding integrins (33-35, 47), the following integrin subunits were selected for further investigation in hDPSCs and SC-hDPSCs: α1, α2, α11 and β1. Integrin β1 was significantly upregulated in SC-hDPSCs (compared to hDPSCs), as confirmed through both immunocytochemistry and western blot analysis. In contrast, no change in expression was observed for the integrin α1 subunit in hDPSCs upon differentiation. Interestingly, a study performed by Rider *et al.* (48) reported that a hMSC subpopulation, FACS sorted for increased expression of integrin α1, displayed enhanced plasticity. This could suggest that the upregulation of integrin α1 is important for maintaining hMSC (and possibly hDPSC) stemness (rather than differentiation). Furthermore, western blot revealed a near 2-fold increase in α11 expression in SC-hDPSCs, although not significant. It is important to notice that integrins are heterodimeric receptors and require both subunits in order to be functionally active and participate in bi-directional signalling pathways. Many processes like cell motility, proliferation, morphology and differentiation are contingent on this continuous dialog between the exterior and interior of the cell (27). Furthermore, the amount of functionally active integrin receptors that is present on the surface of the cell is determined by the amount of α-subunits available (generally, an excess of β subunits exists in the cell) (32, 34). Free α and β subunits do not exist at the cell surface (32). As such, the difference in contractile ability cannot be explained by an increase in β1 protein levels alone. Following the western blot data, integrin α11 (forming a heterodimer with β1) seems to be the most likely candidate to explain the difference in contraction between hDPSCs and SC-hDPSCs. This notion is further supported by a recent study. Popova *et al*. (49) reported that integrin α11 deficieny in mice results in disorganized periodontal ligament formation and tooth-dependent dwarfism. Periodontal ligament is highly enriched with collagen type I and it appears that integrin α11β1 is the only collagen receptor expressed. However, more experiments are necessary to investigate the expression levels of integrin α11 in hDPSCs and SC-hDPSCs (through immunocytochemistry) and its contribution in the contraction process (through antibody-based blocking experiments).

In order to further corroborate the contribution of specific integrin subunits (α1 and β1) in the contraction process of a collagen type I hydrogel, an inhibition experiment was set up. The respective subunits were blocked using specific antibodies (4 different concentrations) after which hDPSCs and SC-hDPSCs were allowed to contract within a collagen type I hydrogel. After 8h, contraction was captured and measured. Blocking of the β1 subunit considerably reduced contraction at the highest concentration, in both hDPSCs and SC-hDPSCs. As could be expected, integrin β1 plays a major role in the contraction process, due to the fact that every collagen-binding receptor incorporates a β1 subunit. On the other hand, blocking of the integrin α1 subunit had no effect whatsoever (not even at high concentrations). This could be explained by the presence of functional redundancy between the α-subunits of collagen type I binding integrins. Research by Popov *et al.* (34) already described a mechanism of compensatory cross-talk between the collagen type I binding integrins in hMSCs, regarding the adhesion to collagen type I. It was observed that the loss of the integrin α1 subunit led to an increased expression of integrin α2 and α11 (as a compensatory mechanism), and loss of integrin α2 stimulated the expression of integrin subunits α1 and α11. Furthermore, knockdown of integrin α11 led to a slight increase only in integrin α1. This resulted in impaired adhesion of hMSCs

to collagen type I (as there hardly is any compensation of other collagen type I binding integrins) (34). Based on these results, it would be interesting to investigate the contraction potential of hDPSCs and SC-hDPSCs after antibody-based blocking of the integrin α11 subunit (and whether or not compensation of other collagen-binding integrin subunits occurs).

Finally, as an additional objective, the myelination potential (through the expression of MBP) of hDPSCs and SC-hDPSCs was investigated. Cells were seeded together with DRG neurons in a collagen type I hydrogel and allowed to incubate for either a short period of time (3 days) or for a longer period (26 days). DRG neurons are pseudounipolar cells frequently used to evaluate neurite outgrowth and myelination. Western blot analysis revealed the exclusive presence of a 17kDa isoform of MBP in the short term samples. However after 26 days, the protein expression levels of the 17kDa isoform had declined, while a 14kDa isoform became apparent in the samples. It is known from the literature that the 14kDa MBP has a plasma membrane distribution (= functionally active form), whereas the 17kDa isoforms are distributed throughout the cytoplasm and nucleus. The latter are thought to be responsible for the upregulated expression of the functionally active myelin isoform that partakes in the formation of myelin sheaths (50). The increase in the amount of functional active MBP (14kDa) could imply that the neurites of DRG neurons were or have been myelinated at that time point

In general, it is important to remark the use of the housekeeping gene beta-actin in our western blot experiments. Beta-actin is used as a loading control, for normalization of the total protein input. Western blot data (for both integrin and myelin expression), however, revealed noticeable differences in the signal intensity of the beta-actin blots between hDPSCs and SC-hDPSCs (for different donors). Beta-actin is a cytoskeletal protein, involved in cell motility, structure and contraction. As such, it could be possible that the expression of the beta-actin protein was altered after Schwann cell differentiation, potentially through integrin-mediated signalling pathways (e.g. members of the Rho family of GTPases have emerged as key regulators of the actin cytoskeleton, coordinated by integrin signalling) (27). In hindsight, it would have been better to use a different housekeeping gene (e.g. GAPDH).

In the present study, SC-hDPSCs have shown to possess a larger contractile potential within a collagen type I hydrogel, compared to hDPSCs. These results were accompanied by a higher expression of the integrin β1 subunit in hDPSCs, as confirmed through both immunocytochemistry and western blot. The importance of β1 in the contraction process was confirmed through inhibition experiments. However, given the heterodimeric nature of integrin receptors, the contribution of specific integrin alpha subunits (e.g. α11) should be explored to reveal the differential contraction potential between hDPSCs and SC-hDPSCs. These results are of high value in the development of self-aligned cellular hydrogels as a neuroregenerative therapy. Controlling the contraction and organization of the cells and matrix will be critical for successfully creating tissue engineered grafts.

5. Conclusion

One of the most important medical breakthroughs of the 20th century was the discovery of stem cells and their remarkable ability to self-renew and differentiate into multiple cell types. Numerous studies have focused on the application of stem cells and tissue engineering to mend and regenerate body structures. In this study, we focused on (SC-)hDPSCs seeded within a collagen type I hydrogel and more specifically the mechanisms mediating their contraction and interaction with the gel. The β1 integrin subunit was shown to play an important role in the contraction of a collagen type I hydrogel in both hDPSCs and SC-hDPSCs. Furthermore, on a protein level, SC-hDPSCs displayed a significant increase in the expression of the β1 subunit, compared to hDPSCs. The increase in integrin β1 alone, however, cannot explain the difference observed between hDPSCs and SC-hDPSCs regarding the contraction of a collagen type I hydrogel. Given the heterodimeric nature of integrin receptors, the contribution of specific integrin alpha subunits should be further explored. Western blot data from our experiments, combined with research in hMSCs, indicate the potential significance of integrin α11. Future studies should further investigate the expression levels of the α11 subunit in hDPSCs and SC-hDPSCs (through immunocytochemistry) and its importance in collagen hydrogel contraction (through antibody-based blocking or knockdown of integrin α11). Results from our study have provided insight in the mechanisms behind cellular self-alignment in collagen type I hydrogel. Furthermore, it provides a basic framework for future studies to further extend the understanding of these interactions. Controlling the contraction and organization of the cells and matrix more effectively will be critical for successfully creating tissue engineered grafts, which can be used to treat large gap PNI.

References

1. Martens W, Bronckaers A, Politis C, Jacobs R, Lambrichts I. Dental stem cells and their promising role in neural regeneration: an update. Clinical oral investigations. 2013;17(9):1969-83.
2. La Noce M, Paino F, Spina A, Naddeo P, Montella R, Desiderio V, et al. Dental pulp stem cells: state of the art and suggestions for a true translation of research into therapy. Journal of dentistry. 2014;42(7):761-8.
3. Weissman IL. Stem cells: units of development, units of regeneration, and units in evolution. Cell. 2000;100(1):157-68.
4. Lakshmipathy U, Verfaillie C. Stem cell plasticity. Blood reviews. 2005;19(1):29-38.
5. Estrela C, Alencar AH, Kitten GT, Vencio EF, Gava E. Mesenchymal stem cells in the dental tissues: perspectives for tissue regeneration. Brazilian dental journal. 2011;22(2):91-8.
6. d'Aquino R, De Rosa A, Laino G, Caruso F, Guida L, Rullo R, et al. Human dental pulp stem cells: from biology to clinical applications. Journal of experimental zoology Part B, Molecular and developmental evolution. 2009;312B(5):408-15.
7. Wagers AJ, Weissman IL. Plasticity of adult stem cells. Cell. 2004;116(5):639-48.
8. Langer R, Vacanti JP. Tissue engineering. Science. 1993;260(5110):920-6.
9. Georgiou M, Bunting SC, Davies HA, Loughlin AJ, Golding JP, Phillips JB. Engineered neural tissue for peripheral nerve repair. Biomaterials. 2013;34(30):7335-43.
10. Phillips JB. Building stable anisotropic tissues using cellular collagen gels. Organogenesis. 2014;10(1):6-8.
11. Li Y, Huang G, Zhang X, Wang L, Du Y, Lu TJ, et al. Engineering cell alignment in vitro. Biotechnology advances. 2014;32(2):347-65.
12. Navarro X, Krueger TB, Lago N, Micera S, Stieglitz T, Dario P. A critical review of interfaces with the peripheral nervous system for the control of neuroprostheses and hybrid bionic systems. Journal of the peripheral nervous system : JPNS. 2005;10(3):229-58.
13. Maravilla KR, Bowen BC. Imaging of the peripheral nervous system: evaluation of peripheral neuropathy and plexopathy. AJNR American journal of neuroradiology. 1998;19(6):1011-23.
14. Gaudet AD, Popovich PG, Ramer MS. Wallerian degeneration: gaining perspective on inflammatory events after peripheral nerve injury. Journal of neuroinflammation. 2011;8:110.
15. Kim HA, Mindos T, Parkinson DB. Plastic fantastic: Schwann cells and repair of the peripheral nervous system. Stem cells translational medicine. 2013;2(8):553-7.
16. Arthur-Farraj PJ, Latouche M, Wilton DK, Quintes S, Chabrol E, Banerjee A, et al. c-Jun reprograms Schwann cells of injured nerves to generate a repair cell essential for regeneration. Neuron. 2012;75(4):633-47.
17. Martens W, Sanen K, Georgiou M, Struys T, Bronckaers A, Ameloot M, et al. Human dental pulp stem cells can differentiate into Schwann cells and promote and guide neurite outgrowth in an aligned tissue-engineered collagen construct in vitro. FASEB journal : official publication of the Federation of American Societies for Experimental Biology. 2014;28(4):1634-43.

18. Lietz M, Dreesmann L, Hoss M, Oberhoffner S, Schlosshauer B. Neuro tissue engineering of glial nerve guides and the impact of different cell types. Biomaterials. 2006;27(8):1425-36.
19. Bozkurt A, Deumens R, Beckmann C, Olde Damink L, Schugner F, Heschel I, et al. In vitro cell alignment obtained with a Schwann cell enriched microstructured nerve guide with longitudinal guidance channels. Biomaterials. 2009;30(2):169-79.
20. Phillips JB, Bunting SC, Hall SM, Brown RA. Neural tissue engineering: a self-organizing collagen guidance conduit. Tissue engineering. 2005;11(9-10):1611-7.
21. Friedenstein AJ. Osteogenetic activity of transplanted transitional epithelium. Acta anatomica. 1961;45:31-59.
22. Gronthos S, Mankani M, Brahim J, Robey PG, Shi S. Postnatal human dental pulp stem cells (DPSCs) in vitro and in vivo. Proceedings of the National Academy of Sciences of the United States of America. 2000;97(25):13625-30.
23. Zuk PA, Zhu M, Ashjian P, De Ugarte DA, Huang JI, Mizuno H, et al. Human adipose tissue is a source of multipotent stem cells. Molecular biology of the cell. 2002;13(12):4279-95.
24. Tuan RS, Boland G, Tuli R. Adult mesenchymal stem cells and cell-based tissue engineering. Arthritis research & therapy. 2003;5(1):32-45.
25. Erices A, Conget P, Minguell JJ. Mesenchymal progenitor cells in human umbilical cord blood. British journal of haematology. 2000;109(1):235-42.
26. Faroni A, Smith RJ, Reid AJ. Adipose derived stem cells and nerve regeneration. Neural regeneration research. 2014;9(14):1341-6.
27. Docheva D, Popov C, Mutschler W, Schieker M. Human mesenchymal stem cells in contact with their environment: surface characteristics and the integrin system. Journal of cellular and molecular medicine. 2007;11(1):21-38.
28. Kopen GC, Prockop DJ, Phinney DG. Marrow stromal cells migrate throughout forebrain and cerebellum, and they differentiate into astrocytes after injection into neonatal mouse brains. Proceedings of the National Academy of Sciences of the United States of America. 1999;96(19):10711-6.
29. Lee JH, Yu HS, Lee GS, Ji A, Hyun JK, Kim HW. Collagen gel three-dimensional matrices combined with adhesive proteins stimulate neuronal differentiation of mesenchymal stem cells. Journal of the Royal Society, Interface / the Royal Society. 2011;8(60):998-1010.
30. Arthur A, Rychkov G, Shi S, Koblar SA, Gronthos S. Adult human dental pulp stem cells differentiate toward functionally active neurons under appropriate environmental cues. Stem cells. 2008;26(7):1787-95.
31. Hynes RO. Integrins: bidirectional, allosteric signaling machines. Cell. 2002;110(6):673-87.
32. Barczyk M, Carracedo S, Gullberg D. Integrins. Cell and tissue research. 2010;339(1):269-80.
33. Heckmann L, Fiedler J, Mattes T, Brenner RE. Mesenchymal progenitor cells communicate via alpha and beta integrins with a three-dimensional collagen type I matrix. Cells, tissues, organs. 2006;182(3-4):143-54.
34. Popov C, Radic T, Haasters F, Prall WC, Aszodi A, Gullberg D, et al. Integrins alpha2beta1 and alpha11beta1 regulate the survival of mesenchymal stem cells on collagen I. Cell death & disease. 2011;2:e186.

35. Foster LJ, Zeemann PA, Li C, Mann M, Jensen ON, Kassem M. Differential expression profiling of membrane proteins by quantitative proteomics in a human mesenchymal stem cell line undergoing osteoblast differentiation. Stem cells. 2005;23(9):1367-77.
36. Majumdar MK, Keane-Moore M, Buyaner D, Hardy WB, Moorman MA, McIntosh KR, et al. Characterization and functionality of cell surface molecules on human mesenchymal stem cells. Journal of biomedical science. 2003;10(2):228-41.
37. Chastain SR, Kundu AK, Dhar S, Calvert JW, Putnam AJ. Adhesion of mesenchymal stem cells to polymer scaffolds occurs via distinct ECM ligands and controls their osteogenic differentiation. Journal of biomedical materials research Part A. 2006;78(1):73-85.
38. Geckil H, Xu F, Zhang X, Moon S, Demirci U. Engineering hydrogels as extracellular matrix mimics. Nanomedicine. 2010;5(3):469-84.
39. Ding F, Wu J, Yang Y, Hu W, Zhu Q, Tang X, et al. Use of tissue-engineered nerve grafts consisting of a chitosan/poly(lactic-co-glycolic acid)-based scaffold included with bone marrow mesenchymal cells for bridging 50-mm dog sciatic nerve gaps. Tissue engineering Part A. 2010;16(12):3779-90.
40. di Summa PG, Kingham PJ, Raffoul W, Wiberg M, Terenghi G, Kalbermatten DF. Adipose-derived stem cells enhance peripheral nerve regeneration. Journal of plastic, reconstructive & aesthetic surgery : JPRAS. 2010;63(9):1544-52.
41. Daly W, Yao L, Zeugolis D, Windebank A, Pandit A. A biomaterials approach to peripheral nerve regeneration: bridging the peripheral nerve gap and enhancing functional recovery. Journal of the Royal Society, Interface / the Royal Society. 2012;9(67):202-21.
42. Gronthos S, Brahim J, Li W, Fisher LW, Cherman N, Boyde A, et al. Stem cell properties of human dental pulp stem cells. Journal of dental research. 2002;81(8):531-5.
43. Martens W, Wolfs E, Struys T, Politis C, Bronckaers A, Lambrichts I. Expression pattern of basal markers in human dental pulp stem cells and tissue. Cells, tissues, organs. 2012;196(6):490-500.
44. Barnabe GF, Schwindt TT, Calcagnotto ME, Motta FL, Martinez G, Jr., de Oliveira AC, et al. Chemically-induced RAT mesenchymal stem cells adopt molecular properties of neuronal-like cells but do not have basic neuronal functional properties. PloS one. 2009;4(4):e5222.
45. Kingham PJ, Kalbermatten DF, Mahay D, Armstrong SJ, Wiberg M, Terenghi G. Adipose-derived stem cells differentiate into a Schwann cell phenotype and promote neurite outgrowth in vitro. Experimental neurology. 2007;207(2):267-74.
46. Vader D, Kabla A, Weitz D, Mahadevan L. Strain-induced alignment in collagen gels. PloS one. 2009;4(6):e5902.
47. Gronthos S, Simmons PJ, Graves SE, Robey PG. Integrin-mediated interactions between human bone marrow stromal precursor cells and the extracellular matrix. Bone. 2001;28(2):174-81.
48. Rider DA, Nalathamby T, Nurcombe V, Cool SM. Selection using the alpha-1 integrin (CD49a) enhances the multipotentiality of the mesenchymal stem cell population from heterogeneous bone marrow stromal cells. Journal of molecular histology. 2007;38(5):449-58.
49. Popova SN, Barczyk M, Tiger CF, Beertsen W, Zigrino P, Aszodi A, et al. Alpha11 beta1 integrin-dependent regulation of periodontal ligament function in the erupting mouse incisor. Molecular and cellular biology. 2007;27(12):4306-16.

50. Pedraza L, Fidler L, Staugaitis SM, Colman DR. The active transport of myelin basic protein into the nucleus suggests a regulatory role in myelination. Neuron. 1997;18(4):579-89.

Auteursrechtelijke overeenkomst

Ik/wij verlenen het wereldwijde auteursrecht voor de ingediende eindverhandeling:
Revealing interactions of differentiated dental pulp stem cells with a collagen type I hydrogel

Richting: **master in de biomedische wetenschappen-klinische moleculaire wetenschappen**
Jaar: **2015**

in alle mogelijke mediaformaten, - bestaande en in de toekomst te ontwikkelen - , aan de Universiteit Hasselt.

Niet tegenstaand deze toekenning van het auteursrecht aan de Universiteit Hasselt behoud ik als auteur het recht om de eindverhandeling, - in zijn geheel of gedeeltelijk -, vrij te reproduceren, (her)publiceren of distribueren zonder de toelating te moeten verkrijgen van de Universiteit Hasselt.

Ik bevestig dat de eindverhandeling mijn origineel werk is, en dat ik het recht heb om de rechten te verlenen die in deze overeenkomst worden beschreven. Ik verklaar tevens dat de eindverhandeling, naar mijn weten, het auteursrecht van anderen niet overtreedt.

Ik verklaar tevens dat ik voor het materiaal in de eindverhandeling dat beschermd wordt door het auteursrecht, de nodige toelatingen heb verkregen zodat ik deze ook aan de Universiteit Hasselt kan overdragen en dat dit duidelijk in de tekst en inhoud van de eindverhandeling werd genotificeerd.

Universiteit Hasselt zal mij als auteur(s) van de eindverhandeling identificeren en zal geen wijzigingen aanbrengen aan de eindverhandeling, uitgezonderd deze toegelaten door deze overeenkomst.

Voor akkoord,

Luyck, Sander

Datum: **20/01/2015**